ChemComm

COMMUNICATION

View Article Online
View Journal | View Issue

Cite this: *Chem. Commun.*, 2023, 59, 10512

Received 19th June 2023,
Accepted 10th July 2023

DOI: 10.1039/d3cc02929h

rsc.li/chemcomm

Aqueous colloidal nanoplatelets for imaging and improved ALA-based photodynamic therapy of prostate cancer cells†

Kubra Onbasli, ‡[a] Gozde Demirci,[a] Furkan Isik,[b] Emek Goksu Durmusoglu,[c] Hilmi Volkan Demir *[bc] and Havva Yagci Acar *[ade]

Fluorescent, CdSe/CdS core/crown heterostructured nanoplatelets (NPLs) were transferred to the water *via* a simple, single-step ligand exchange using 2-mercaptopropionic acid in a simple extraction process. These stable, aqueous NPLs were loaded with a modal drug, 5-aminolevulinic acid (ALA). ALA-loaded NPLs emerged as a new class of theranostic nanoparticles for image-guided enhanced photodynamic therapy of both androgen-dependent and -independent human prostate cancer cells.

The last decade has seen atomically-flat semiconductor nanocrystals, commonly referred to as nanoplatelets (NPLs) or alternatively known as colloidal quantum wells (CWQs), emerging as an excellent class of quantum emitter colloids. NPLs have been widely exploited in various soft optoelectronic platforms, including light-emitting diodes (LEDs),[1,2] lasers,[3] displays,[4] and energy-harvesting devices.[5] Only recently, there is an increasing interest in their potential biomedical applications triggered by the superior properties that NPLs offer over conventional colloidal quantum dots (CQDs).[6,7] Among these advantages of NPLs are extra-ordinarily large absorption cross-sections, giant oscillator strength (leading into strong absorbers/emitters) and suppressed inhomogeneous broadening (providing sharp emitters with ultra-narrow emission bandwidth).[8] Moreover, through the design and synthesis of NPL heterostructures, high levels of stability (chemical, photo, and thermal) can further be attained, and emissive properties can be additionally engineered to target certain applications, *e.g.*, using core/crown and/or core@shell structures, where the former is obtained by anisotropic growth of a secondary structure only on the periphery of NPLs without changing the total thickness and the latter, by the total encapsulation of NPLs in a secondary structure *via* isotropic growth.[9,10] Among the emissive properties, one of the main achievements of such heterostructured NPLs is their ability to sustain their quantum yield (QY) profoundly high compared to that of the only-core seeds, even when ligand-exchanged or in non-native media, by strongly passivating their surface trap sites, which otherwise lead to nonradiative recombination competing with radiative processes.[11]

The typical synthesis of NPLs is performed in noncoordinating organic solvents; hence, the as-synthesized NPLs are stabilized with ligands with hydrophobic tails.[12] That is why transferring NPLs into the water phase, preferably *via* a facile, single-step process producing colloidally stable aqueous NPLs, is key to any biomedical application. There are a few previous attempts in the literature on preparing such aqueous NPLs for cell labelling and bioimaging. Lim *et al.* transferred CdSe/CdS core/shell NPLs to water using a lipoprotein coating (L-NPLs) as the first example of aqueous NPLs prepared for biological applications to improve their internalization by A431 cells displaying intracellular fluorescence.[6] This approach required a two-step coating wherein first phospholipids were deposited on the NPLs and then coated with amphipathic membrane scaffold proteins in the presence of detergents, which is a relatively tedious procedure. Radchanka *et al.* encapsulated CdSSe@ZnCdS core@shell NPLs with amphiphilic zwitterionic polymer (modified poly(maleic anhidride-*alt*-tetradecene)) and showed their potential in cell labelling (glioma C6 cells) and two-photon imaging.[7] Similarly, Halim *et al.* utilized an amphiphilic

[a] *Department of Chemistry, Koc University, Rumelifeneri Yolu, Sariyer, Istanbul, 34450, Turkey. E-mail: fyagci@ku.edu.tr*
[b] *Department of Electrical and Electronics Engineering, Department of Physics, UNAM-Institute of Materials Science and Nanotechnology, Bilkent University, Ankara 06800, Turkey. E-mail: volkan@fen.bilkent.edu.tr*
[c] *LUMINOUS! Centre of Excellence for Semiconductor Lighting and Displays, The Photonics Institute, School of Electrical and Electronic Engineering, School of Physical and Mathematical Sciences, School of Materials Science and Engineering, Nanyang Technological University, Singapore 639798, Singapore*
[d] *Graduate School of Materials Science and Engineering, Koc University, Rumelifeneri Yolu, Sariyer, Istanbul 34450, Turkey*
[e] *KUYTAM, Koc University Surface Science and Technology Center, 34450 Istanbul, Turkey*

† Electronic supplementary information (ESI) available. See DOI: https://doi.org/10.1039/d3cc02929h

‡ Current address: Department of Metallurgical and Materials Engineering, Istanbul Technical University, 34469, Istanbul, Turkey.

polymer (dodecyl-grafted poly(isobutylene-*alt*-maleic acid)), which is bound to the NPL surface *via* hydrophobic interactions between the dodecyl grafts and the long hydrocarbon chains of oleic acids attached to the surface of the NPLs as stabilizing ligands.[13] These NPLs were internalized by RAW264.7 cells and exhibited intracellular fluorescence. In all of these previous reports, evaluation of the biomedical use of such NPLs has been limited to fluorescent labelling of cells. The demonstration of aqueous NPLs as an optically-trackable drug delivery vehicle is lacking.

In this work, we both aimed a simple, single-step transfer of NPLs to aqueous media and a demonstration of such aqueous NPLs as theranostic nanoparticles for image-guided photodynamic therapy (PDT).

Here, we first synthesized hydrophobic CdSe/CdS core/crown heterostructured NPLs with sharp green emission following our previously reported method. These NPLs coated with oleic acid were successfully transferred from hexane into the water *via* a single step ligand-exchange using 2-mercaptopropionic acid (2MPA) as described in Fig. 1. We have previously shown the superiority of 2MPA in providing excellent stability and stronger emission to commonly used 3MPA in the case of colloidal CdS and CdTe quantum dots.[14] These 2MPA-NPLs have small hydrodynamic sizes (19.14 nm), suggesting successful ligand-exchange with no significant agglomeration and a negative surface charge with high zeta potential (−46.1 mV), favouring colloidal stability. Transfer of NPLs from hexane to water caused a 30 nm red-shift in PL maximum (515 to 545 nm), which was accompanied by about 20 nm red-shift in the heavy and light holes peaks in the absorbance spectra (Fig. S1, ESI†). This is due to the relatively strong bonding between surface cadmium atoms of NPLs and sulfur atoms in 2MPA, which relaxes the quantum confinement in the direction of thickness to some extent. Additionally, as a result, the full-width-at-half-maximum slightly increased from 10 to 23 nm. Also, we observed a slight quantum yield loss from 40% to 13% after the ligand-exchange process, but this is still strong emission for intracellular imaging. Dark field transmission electron microscopy images in Fig. S1c and d (ESI†), reveal there is no change in the shape of NPLs before and after the ligand-exchange. Rectangular-shaped CdSe/CdS NPLs have average lengths of 31.83 ± 2.7 nm and 15.15 ± 1.8 nm for *x*- and *y*-dimensions (Fig. S2, ESI†).

Next, cytocompatibility and potential as intracellular optical probes of these 2MPA-NPLs were tested on three prostate cancer (PCa) cells (LNCaP, PC3, DU145) and a healthy prostate cell line (PNT1A) (Fig. S3, ESI†).

Although any cancer type may be used, PCa cell lines were used in the *in vitro* testing of the hypothesis here. Prostate cancer is the second most frequent cancer diagnosed globally and the fifth cancer-related death in men.[15] Our group studied chemo/photothermal therapy (PTT) combination on androgen-dependent and independent PCa cells using superparamagnetic iron oxide nanoparticles as a drug delivery vehicle and PTT agent.[16]

Cells treated with 2MPA-NPLs between 5–100 μg Cd mL^{-1} concentration showed no loss in viability, suggesting these NPLs are non-toxic in the studied range (Fig. S3, ESI†). Luminescence of 2MPA-NPL (50 μg Cd mL^{-1}) allowed the tracking of time and cell type-dependent internalization of the NPLs (Fig. S4, ESI†). Intracellular green luminescence increased in all cell types with an increasing incubation time of the 2MPA-NPLs

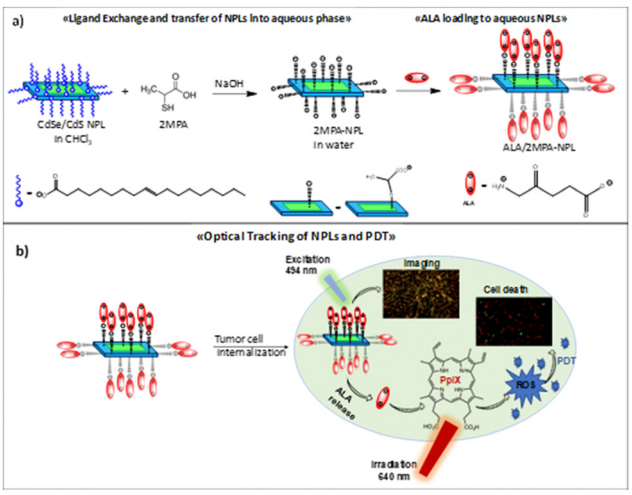

Fig. 1 (a) Design of stable, aqueous, ALA loaded NPLs and (b) its utilization for *in vitro* fluorescent imaging and image-guided ALA-based PDT.

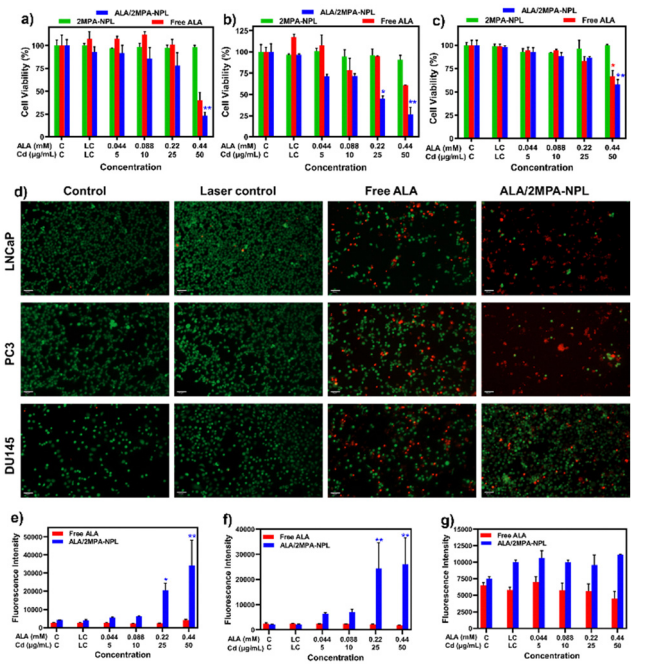

Fig. 2 Influence of free ALA, 2MPA-NPL, and ALA/2MPA-NPL on the viability of (a) LNCaP, (b) PC3, and (c) DU145 cells as determined by MTT at different concentrations, (d) images of stained LNCaP, PC3, and DU145 cells with live/dead assay kit at 0.44 mM ALA or 50 μg Cd mL^{-1} concentration, ROS production in free ALA and ALA/2MPA-NPL treated (e) LNCaP, (f) PC3, and (g) DU145 cells after LED irradiation. All irradiation experiments were performed using 640 nm LED at 10 mW cm^{-2} for 3 min after 4 h incubation. Untreated cells were used as control. Data are expressed as mean ± SD (n = 3). Scale bars = 85 μm.

with the cells, suggesting increasing cellular uptake, as expected. Short incubation time (4 h) differentiated the cell types: PC3 cells quickly picked up the 2MPA-NPLs, followed by LNCaP cells. The slowest uptake was observed in DU145 cells. These results indicate that these cytocompatible 2MPA-NPLs have the potential as imaging/tracking agents.

Towards demonstration of 2MPA-NPLs' theranostic potential, zwitterionic 5-aminolevulinic acid (ALA) is used as a model drug to induce enhanced PDT *via* improved delivery of ALA to cancer cell lines utilizing NPLs as a delivery vehicle. ALA-PDT has become popular lately, after its FDA approval.[17–19] PDT offers appreciable locality to the treatment, does not cause cumulative toxicity and may activate the immune system. ALA is indeed a prodrug that is converted to a photosensitizer, protoporphyrin IX (PpIX), intracellularly and produces reactive oxygen species (ROS) when irradiated at 400 or 630 nm using a LED or a laser to induce cell-death.[20,21] ALA conversion to PpIX is usually faster and more in tumor cells, which brings in a level of tumor specificity. However, due to its zwitterionic nature, its low bioavailability limits its use in the clinic.[22] Previously, we successfully delivered ALA to tumor cells *via* nanoparticles, which effectively lowered the active dose and improved phototoxicity.[23] In addition, ALA may offer some selectivity between different cancer cells based on PEPT1/PEPT2 expression and, hence, may also be considered as a targeting moiety. PEPT1 and PEPT2 are membrane transporter proteins mediating proton-dependent cellular uptake of oligopeptides and some drugs.[24]

ALA (2.56 mg) was loaded to 2MPA-NPLs (12.8 mg) *via* electrostatic interaction in water which was confirmed by isothermal titration calorimetry (Fig. S5, ESI†). After ALA loading, the hydrodynamic size increased to 21.74 nm, and the zeta potential was reduced to −26.2 mV. Dose-dependent dark cytotoxicity of ALA/2MPA-NPLs (5–100 μg Cd mL^{-1}) and free ALA (0.044–0.88 mM) at the equivalent dose of the ALA content of ALA/2MPA-NPL was determined after 24 h incubation with the cells using standard MTT assay (Fig. S3, ESI†). Slight dark toxicity was observed only with ALA/2MPA-NPL, reducing the viability of LNCaP (Fig. S3a, ESI†) and DU145 (Fig. S3c, ESI†) to 75.8% and 77%, respectively, at the highest studied dose (100 μg Cd mL^{-1} and 0.88 mM ALA). All other doses and free ALA were safe in all cell lines. The internalization of free ALA, 2MPA-NPL, and ALA/2MPA-NPL by PCa cells were determined by fluorescence microscopy after 4 h and 24 h incubation at 0.44 mM ALA or 50 μg Cd mL^{-1} dose (Fig. S4, ESI†). Short incubation time gives information about the selectivity of agents towards different cell lines. At the end of 4 h incubation, a significant amount of green fluorescence was observed in PC3 cells, which increased with the incubation time (24 h) (Fig. S4, ESI†), but not in LNCaP and DU145 cells, suggesting a preferential uptake of 2MPA-NPLs by PC3 cells. Free ALA, which is converted to red fluorescent PpIX in the cells, also accumulated in PC3 cells in the greatest amount, followed by LNCaP. In the case of the DU145 cells, no appreciable internalization of 2MPA-NPLs or free ALA was observed at short incubation, but a significant PpIX signal was observed after a long incubation time. PpIX signal increased in all cell lines with the preserved cell-type difference after 24 h incubation. Indeed, ALA was reported to target LNCaP and PC3 cells but not DU145 cells, based on PEPT1/PEPT2 targeting; hence this observation is in agreement with the literature and was expected since ALA is on the surface of the NPLs.[24,25] But, a synergistic enhancement in the cellular uptake was observed in all cell types, demonstrating ALA-based selectivity as well as improved delivery of ALA *via* NPLs (Fig. S4, ESI†).

Next, ALA-PDT of androgen-dependent LNCaP and androgen-independent PC3 and DU145 cells were investigated. Phototoxicities of free ALA, 2MPA-NPL, and ALA/2MPA-NPL were evaluated on PCa cells at four different concentrations after 3 min 640 nm LED irradiation (10 mW cm^{-2}). Cells were treated with NPLs for 4 h and 24 h, between 5–50 μg Cd mL^{-1}, and free ALA between 0.044–0.88 mM, equivalent to ALA content of ALA/2MPA-NPL. Both MTT and live/dead assay showed that the laser irradiation itself did not cause any cell death (Fig. 2a–d) and (Fig. S6, ESI†). Live cells were determined based on esterase activity, tracked by green fluorescent calceine-AM staining of the live/dead assay. No cell death was observed due to 2MPA-NPL + LED treatment after 4 h or 24 h incubation, indicating that NPLs do not cause phototoxicity under the studied conditions and are safe delivery/imaging agents. Free ALA showed significant phototoxicity only at the highest concentration and most effective in the following order: LNCaP, PC3, and DU145 with 40-61-66% viable cell count. This agrees with the PpIX levels observed by fluorescence microscopy (Fig. S4, ESI†).

In the case of ALA/2MPA-NPL treated LNCaP cells, significant cell death was observed at 50 μg Cd mL^{-1}–0.44 mM ALA reducing viability to 23.3% (Fig. 2a). A dramatic difference between the phototoxicity of free ALA and ALA/2MPA-NPL was observed on the PC3 cell line (Fig. 2b). Significant toxicity was observed at 0.22 mM ALA equivalent concentration of ALA/2MPA-NPLs, while free ALA at this dose did not cause any phototoxicity. At the highest dose (0.44 mM ALA), viability dropped to 61% with free ALA but to 26% with ALA/2MPA-NPL, suggesting better delivery of ALA to cells *via* NPLs, as observed in Fig. S4 (ESI†). Phototoxicity in DU145 cells was observed only at the highest dose, but the therapeutic effect was weaker than in the other two cells. Only 66.7% of DU145 cells were viable after ALA + LED and 58.3%, after ALA/2MPA-NPLs + LED, respectively (Fig. 2c).

Live/dead cell viability assay was performed after 4 h incubation at 0.44 mM ALA or 50 μg Cd mL^{-1} on each cell line to confirm MTT results (Fig. 2d). Red fluorescence from ethidium homodimer-1 shows cells that lost their plasma membrane integrity. Fluorescence microscopy images of cells treated with ALA/2MPA-NPL + LED indicated a large number of dead cells (red) in LNCaP and PC3 cells and less in DU145 cells, in agreement with MTT results.

Phototoxicity increased dramatically after 24 h incubation of cells with free ALA and ALA/2MPA-NPL, as internalization increases with time (Fig. S6, ESI†). In LNCaP and PC3 cells, almost complete cell death was observed at 0.22 and 0.44 mM ALA (25 and 50 μg Cd mL^{-1}) after laser irradiation of free ALA or ALA/2MPA-NPL. The viability of DU145 cells was 50% and 38.5% after the laser irradiation of free ALA and ALA/2MPA-NPL, respectively at 0.44 mM or 50 μg Cd mL^{-1}.

ROS triggers cell death in PDT. Intracellular, dose-dependent ROS generation was investigated using a cell-permeable ROS sensor, 2′,7′-dichlorofluorescein diacetate ($DCFH_2$-DA) in treated PCa cells (Fig. 2e–g). A dramatically higher level of intracellular ROS production with ALA/2MPA-NPL + LED compared to free ALA, especially at 0.22–0.44 mM ALA was determined in LNCaP and PC3 cells (Fig. 2e and f). The impact of ALA/2MPA-NPL based treatment increased the intracellular ROS levels in DU145 cells, as well, but in much lower amounts (Fig. 2g). Overall, determined ROS levels correlate with the phototoxicity observed in these cell lines.

In this work, we transferred core/crown CdSe/CdS NPLs from hexane to water *via* a facile single-step ligand-exchange using 2MPA for ALA-based PDT of both androgen-dependent, LNCaP and -independent, PC3 and DU145 prostate cancer cells. Aqueous NPLs were electrostatically loaded with ALA to deliver the prodrug to PCa cells effectively. 2MPA-NPLs caused no significant toxicity on PCa or healthy prostate cell lines. Moreover, strong intracellular green luminescence proved these NPLs as excellent optical probes, which shows faster internalization by PC3 cells. ALA also showed differential internalization, favoring PC3, followed by LNCaP. ALA also showed differential internalization, which is suggested by decreasing amount of PpIX-red fluorescence, favouring PC3, followed by LNCaP, and only weak red fluorescence in DU145 cells suggesting weaker internalization of ALA by DU145. This trend suggests a level of specific targeting of PC3 and LNCaP cells. This provided a synergistic theranostic effect. ALA loading on 2MPA-NPLs improved internalization by LNCaP and PC3 cells dramatically, leading to enhanced PpIX formation resulting in stronger phototoxicity of ALA/2MPA-NPLs compared to free ALA, evidenced by 40–50% lower viability. Dramatically higher intracellular ROS generation on LNCaP and PC3 cells with ALA/2MPA-NPLs + LED confirmed effective PDT driving cells to death. Almost complete cell death was observed on LNCaP and PC3 cells with both free ALA and ALA/2MPA-NPL after a long incubation time at 0.22–0.44 mM ALA, where passive cell uptake increased significantly. It is important to note that 2MPA-NPLs did not cause any phototoxicity under the same conditions, proving them as a very promising optically trackable delivery vehicle for photosensitizers. These findings suggest the higher accumulation of ALA in the cells *via* NPLs, and although further investigations may be necessary, a degree of cell selectivity of ALA/2MPA-NPLs due to surface ALA towards PEPT1/PEPT2. Overall, this study suggested that 2MPA-NPLs could be used as a safe and promising agent for image-guided PDT of prostate cancer cells. On the other hand, these aqueous NPLs may be exploited for the delivery of other drugs or utilized in the treatment of other cancer types.

FI synthesized and characterized oleic acid coated NPLs; GD and KO prepared and characterized the aq. NPLs, performed all *in vitro* tests; EGD, HVD, KO and HYA conceptualized the project, and contributed to data interpretation and manuscript preparation.

KO thanks Koc University Seed Fund for the financial support. HVD also acknowledges the support from TÜBA.

Conflicts of interest

There are no conflicts to declare.

Notes and references

1 Y. Altintas, B. Liu, P. L. Hernández-Martínez, N. Gheshlaghi, F. Shabani, M. Sharma, L. Wang, H. Sun, E. Mutlugun and H. V. Demir, *Chem. Mater.*, 2020, **32**, 7874–7883.
2 B. Liu, Y. Altintas, L. Wang, S. Shendre, M. Sharma, H. Sun, E. Mutlugun and H. V. Demir, *Adv. Mater.*, 2020, **32**, 1905824.
3 M. Wu, S. T. Ha, S. Shendre, E. G. Durmusoglu, W.-K. Koh, D. R. Abujetas, J. A. Sánchez-Gil, R. Paniagua-Domínguez, H. V. Demir and A. I. Kuznetsov, *Nano Lett.*, 2020, **20**, 6005–6011.
4 T. Erdem and H. V. Demir, *Nanophotonics*, 2016, **5**, 74–95.
5 M. Sharma, K. Gungor, A. Yeltik, M. Olutas, B. Guzelturk, Y. Kelestemur, T. Erdem, S. Delikanli, J. R. McBride and H. V. Demir, *Adv. Mater.*, 2017, **29**, 1700821.
6 S. J. Lim, D. R. McDougle, M. U. Zahid, L. Ma, A. Das and A. M. Smith, *J. Am. Chem. Soc.*, 2016, **138**, 64–67.
7 A. Radchanka, A. Iodchik, T. Terpinskaya, T. Balashevich, T. Yanchanka, A. Palukoshka, S. Sizova, V. Oleinikov, A. Feofanov and M. Artemyev, *Nanotechnology*, 2020, **31**, 435102.
8 S. Ithurria, M. Tessier, B. Mahler, R. Lobo, B. Dubertret and A. L. Efros, *Nat. Mater.*, 2011, **10**, 936–941.
9 M. D. Tessier, P. Spinicelli, D. Dupont, G. Patriarche, S. Ithurria and B. Dubertret, *Nano Lett.*, 2014, **14**, 207–213.
10 A. Robin, E. Lhuillier and B. Dubertret, *MRS Adv.*, 2016, **1**, 2187–2192.
11 D. Dede, N. Taghipour, U. Quliyeva, M. Sak, Y. Kelestemur, K. Gungor and H. V. Demir, *Chem. Mater.*, 2019, **31**, 1818–1826.
12 J. Zhang, Y. Sun, S. Ye, J. Song and J. Qu, *Chem. Mater.*, 2020, **32**, 9490–9507.
13 H. Halim, J. Simon, I. Lieberwirth, V. Mailänder, K. Koynov and A. Riedinger, *J. Mater. Chem. B*, 2020, **8**, 146–154.
14 R. Kas, E. Sevinc, U. Topal and H. Y. Acar, *J. Phys. Chem. C*, 2010, **114**, 7758–7766.
15 H. Sung, J. Ferlay, R. L. Siegel, M. Laversanne, I. Soerjomataram, A. Jemal and F. Bray, *CA-Cancer J. Clin.*, 2021, **71**, 209–249.
16 K. Onbasli, M. Erkısa, G. Demirci, A. Muti, E. Ulukaya, A. Sennaroglu and H. Y. Acar, *Biomater. Sci.*, 2022, **10**, 3951–3962.
17 K. Bilici, S. Cetin, E. Aydındogan, H. Yagci Acar and S. Kolemen, *Front. Chem.*, 2021, 444.
18 B. Krammer and K. Plaetzer, *Photochem. Photobiol. Sci.*, 2008, **7**, 283–289.
19 A. Punjabi, X. Wu, A. Tokatli-Apollon, M. El-Rifai, H. Lee, Y. Zhang, C. Wang, Z. Liu, E. M. Chan and C. Duan, *ACS Nano*, 2014, **8**, 10621–10630.
20 J. Wu, H. Han, Q. Jin, Z. Li, H. Li and J. Ji, *ACS Appl. Mater. Interfaces*, 2017, **9**, 14596–14605.
21 A. Casas, *Cancer Lett.*, 2020, **490**, 165–173.
22 R. F. Donnelly, P. A. McCarron and D. A. Woolfson, *Perspect. Med. Chem.*, 2007, **1**, 1177391X0700100005.
23 M. Hashemkhani, M. Loizidou, A. J. MacRobert and H. Yagci Acar, *Inorg. Chem.*, 2022, **61**, 2846–2863.
24 W. Tai, Z. Chen and K. Cheng, *Mol. Pharm.*, 2013, **10**, 477–487.
25 L. Rodriguez, A. Batlle, G. Di Venosa, A. J. MacRobert, S. Battah, H. Daniel and A. Casas, *Int. J. Biochem. Cell Biol.*, 2006, **38**, 1530–1539.